

## The role of gas composition in plasma-dust structures in RF discharge

S. A. Maiorov, S. K. Kodanova, M. K. Dosbolayev, T. S. Ramazanov, R. I. Golyatina, N. Kh. Bastykova, and A. U. Utegenov

Citation: *Physics of Plasmas* (1994-present) **22**, 033705 (2015); doi: 10.1063/1.4916566

View online: <http://dx.doi.org/10.1063/1.4916566>

View Table of Contents: <http://scitation.aip.org/content/aip/journal/pop/22/3?ver=pdfcov>

Published by the [AIP Publishing](#)

---

### Articles you may be interested in

[Observation of  \$\Omega\$  mode electron heating in dusty argon radio frequency discharges](#)

*Phys. Plasmas* **20**, 083704 (2013); 10.1063/1.4818442

[Agglomeration processes sustained by dust density waves in Ar / C<sub>2</sub>H<sub>2</sub> plasma: From C<sub>2</sub>H<sub>2</sub> injection to the formation of an organized structure](#)

*Phys. Plasmas* **20**, 033703 (2013); 10.1063/1.4796047

[Investigation of plasma-dust structures in He-Ar gas mixture](#)

*Phys. Plasmas* **15**, 093701 (2008); 10.1063/1.2977763

[Dust grains as a Diagnostic Tool for RF-Discharge Plasma](#)

*AIP Conf. Proc.* **669**, 90 (2003); 10.1063/1.1593873

[Dust grains as a diagnostic tool for rf-discharge plasma](#)

*AIP Conf. Proc.* **649**, 325 (2002); 10.1063/1.1527790

---



## The role of gas composition in plasma-dust structures in RF discharge

S. A. Maiorov,<sup>1,2,a)</sup> S. K. Kodanova,<sup>3</sup> M. K. Dosbolayev,<sup>3</sup> T. S. Ramazanov,<sup>3</sup> R. I. Golyatina,<sup>1</sup> N. Kh. Bastykova,<sup>3</sup> and A. U. Utegenov<sup>3</sup>

<sup>1</sup>*Prokhorov General Physics Institute, Russian Academy of Sciences, Vavilov st. 38, Moscow 119991, Russia*

<sup>2</sup>*Joint Institute for High Temperatures, Russian Academy of Sciences, Izhorskaya st. 13/19, Moscow 127412, Russia*

<sup>3</sup>*Institute of Experimental and Theoretical Physics, Al-Farabi Kazakh National University, Al-Farabi 71, Almaty 050040, Kazakhstan*

(Received 30 December 2014; accepted 16 March 2015; published online 30 March 2015)

The influence of a mixture of light and heavy gases, i.e., helium and argon, on plasma-dust structures in the radiofrequency discharge has been studied. The dust chains in the sheath of the radiofrequency discharge, the average distance between the dust particles and their chains, have been analyzed. A significant effect of small amounts of argon on the correlation characteristics of dust particles has been observed. The results of numerical simulation of ion and electron drift in the mixture of helium and argon are presented. It is shown that even 1% of argon admixture to helium produces such an effect that argon ions become the main components of the discharge, as they drift with lightweight helium forming a strongly anisotropic velocity distribution function.

© 2015 AIP Publishing LLC. [<http://dx.doi.org/10.1063/1.4916566>]

### I. INTRODUCTION

Drift in a strong electric field can be accompanied by considerable heating of ions, and in case of a large difference in atomic masses of ions and atoms, the ion distribution function may have a high degree of anisotropy. As the anisotropy of the ion distribution function can, in turn, cause a significant change in properties of dust structures in plasma, the idea of experiments with dusty plasma in the discharge in the mixture of light and heavy gases, i.e., helium and xenon, was proposed.<sup>1</sup> The results of calculations for the mixture of easily ionized heavy gases (and, probably, vapors of heavy metals, i.e., mercury, cesium and some others, see a more detailed analysis in Refs. 2 and 3), make it possible to predict a strong effect of gas composition on the characteristics of plasma–dust structures in discharges. More precisely, a discharge in the mixture with a low concentration of easily ionized heavy gas may acquire features caused by the supersonic nature of the flux, i.e., the Mach cone, anisotropy of the interaction of dust particles, and others.

A small admixture to the working gases can cause a considerable (and uncontrollable) change in the discharge properties. No due importance is given to this circumstance when analyzing experimental data, though observation of the discharge for a few minutes after its ignition shows changes in the glow behavior, which can be caused, e.g., by selection of ions and atoms in the discharge.

Dust structures in the helium–argon mixture at a low concentration of the latter were studied in Refs. 4 and 5; structures in the helium–krypton mixture were studied in Ref. 6 and the discharge in the helium–xenon mixture with a longitudinal magnetic field was studied in Ref. 7.

As expected, the discharge in mixtures of atoms with very different atomic masses offers new possibilities for

formation of dust structures in the gas discharge. Due to the decrease in the concentration of intrinsic gas atoms, the frequency of ion–atom collisions with resonant charge exchange abruptly decreases, hence, the ion mean free path increases. Accordingly, the discharge parameters will also be different, i.e., the increase in the ion drift velocity and the diffusion coefficient causes a decrease in the ion density due to rapid ion drift to walls.

Another interesting possibility of controlling the ion flux characteristics is formation of a light ion drift among heavy atoms (see Ref. 2). For dusty plasma, this means:

- (1) suppression of the ion drag force exerted on a dust particle by ions;
- (2) decrease in ion heating due to a significant decrease in the drift velocity.

In studying of dust structures in the hydrogen–argon mixture,<sup>8</sup> characteristics unusual for dusty plasma were obtained, which can be directly associated with these effects.

Ion drag force arises when there is a difference between the average velocity of ions and dust particles associated with the transfer of momentum. The ion drag considerably affects the location and configuration of dust structures in the laboratory plasma devices,<sup>9</sup> it is responsible for rotation of dust particles in the presence of a magnetic field,<sup>10</sup> initiates void formation,<sup>11</sup> and influences the dispersion of dust in the low-frequency plasma waves.<sup>12</sup>

The influence of ion-atom collisions and closely located dust grains on such processes as dust charging and ion drag is well known.<sup>13</sup> In particular, ion-atom collisions can cause the difference of the ion distribution function from the Maxwellian distribution. Collisions with charge exchange between ions and atoms can lead to a new kind of forces.<sup>14</sup>

In the experimental works,<sup>15–17</sup> the influence of the wake field on the structural properties of dusty plasma was investigated. To study the role of the ion flux (focus) in

<sup>a)</sup>Electronic mail: maiorov\_sa@mail.ru

formation of the vertical chain of dust particles, the authors used a special trap in the discharge of a homogeneous gas. In this paper, we present the results of experimental and theoretical investigations of the influence of plasma composition on the structural properties of plasma-dust formations.

In the experiment, a mixture of helium and argon, with 97% concentration of light atoms (helium), was used as the plasma-forming gas, whereas pure helium and argon were used to compare the obtained results with those for pure gases. The choice of such a gas mixture is explained by high ratio of atomic masses of chosen gases, and, thus, a possibility to observe either a significant influence of the ion flux or a proportional distribution of gas molecules in the plasma-dust formations.

## II. RESULTS OF EXPERIMENTS

### A. Experimental setup

The experiments were carried out in a conventional gas discharge setup. The main part of the experimental setup was the electrode system producing a high-frequency capacitive gas discharge. Disk electrodes of 100 mm diameter were placed parallel to each other in the horizontal plane at a distance of 30 mm. The upper electrode was grounded and had a small hole used for dust injection into the plasma and for video-shooting. The dust particles were illuminated by a 0.4 mm laser knife, which enabled experimenters to obtain cross sections of plasma-dust structures. The trajectories of dust particles were registered by high-speed video camera with frame frequencies up to 300 frames per second. The lower electrode was connected to the RF generator providing signals with a frequency  $f = 13.56$  MHz.<sup>18</sup> In the experiments, hollow spherical dust particles of average diameter of

20–40  $\mu\text{m}$  were used. To prevent escape of the dust particles in the radial direction, the annular trap was used. In all experiments, the power supplied by the high frequency generator was equal to 16 W.

### B. Experimental results

During the discharge in pure gases and He/Ar mixture, the dust structures were formed, which were confined in the lower sheath traps. To study the dependence of interparticle distances and pair correlation distribution functions of dust particles on gas pressure and gas percentage, the experiments with pure gases, i.e., helium and argon, and argon mixture at a content of 3% were performed. Figure 1 shows typical dust structures at a pressure of 0.3 Torr. Figures 1(a) and 1(b) correspond to the top view in pure helium and in helium-argon mixture, respectively. Figures 1(c) and 1(d) show side views of the same structures. Figures 2 and 3 show pair correlation functions for dust particles  $g(r/a)$  ( $a$  is the Wigner-Seitz radius), which determine the relative probability of finding a particle at a distance  $r$  from the other particle. It means that by the value of the ratio between the first and the second peaks, it is possible to determine the type of bond between particles, for example, Figure 2 shows that at a relatively low pressure (0.28 Torr), the dust structure is in a liquid phase. However, as the pressure increases, the coupling between particles becomes stronger, and at sufficiently high pressures (1.01 Torr) particles have a liquid-crystal structure. The comparison of Figures 2 and 3 shows that an addition of a heavy gas to the light one causes significant changes in the properties of dust structures. At a low pressure (0.25 Torr) in the helium-argon (Ar—3%) gas mixture, significant oscillations in the curve of the pair correlation function are observed,

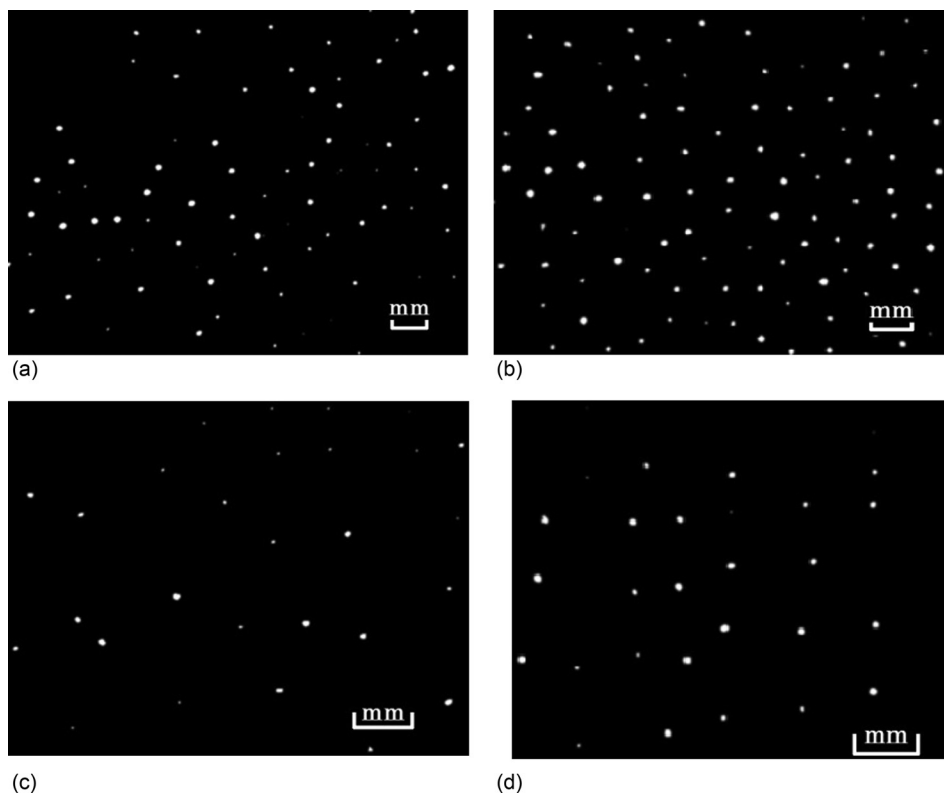


FIG. 1. Top view (a), (b) and side view (c), (d) of dust structures in pure helium and in the mixture of He (97%) + Ar (3%) at a gas pressure of 0.3 Torr. a- (He), b- (He+Ar), c- (He); d- (He+Ar).

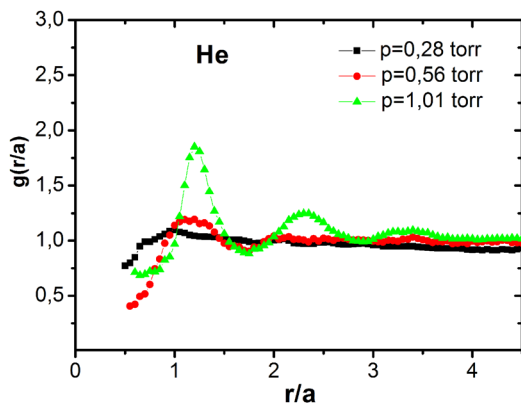


FIG. 2. Pair correlation functions of dust particles in pure helium at different pressures.

which indicate formation of a liquid crystal dust structure. Figure 4 shows that at a rather low pressure of mixture and argon, dust particles have a liquid-crystal structure, whereas under the same conditions in the helium plasma, the dust has gaseous structure.

Figure 5 shows the dependence of the average distance between particles on the gas pressure. The distances between the closest particles are determined by the analysis of the pair correlation function. The images of dust particles are considered separately in the horizontal and vertical planes. In both cases, the dust system was illuminated by a laser knife of 0.4 mm thickness.

The analysis of these dependencies shows that:

- (1) In the horizontal plane, the average distance between dust particles weakly depends on the gas pressure and is, practically, the same in pure helium and mixture of He+Ar;
- (2) In pure helium, the mean distance between dust particles along the chains (which is shown by a vertical plane) sharply decreases with increasing pressure;
- (3) The mean distance between dust particles along the chains in the gas mixture is much shorter than that in the pure gas, in addition, it considerably decreases with increasing pressure.

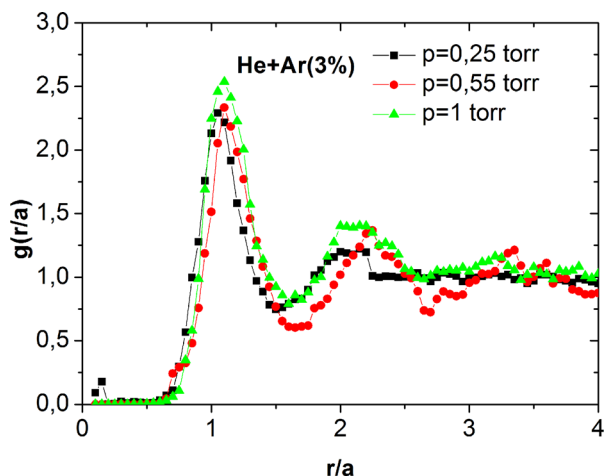


FIG. 3. Pair correlation functions of dust particles in the mixture of helium (97%) and argon (3%) at different pressures.

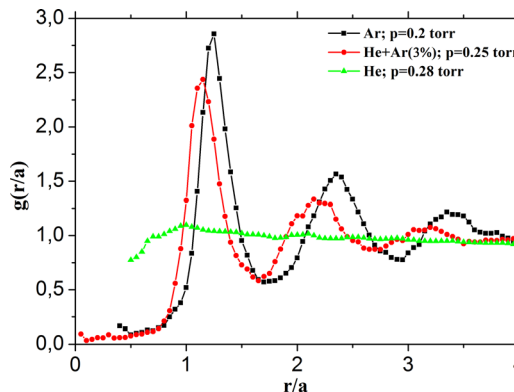


FIG. 4. Pair correlation functions of dust particles in pure argon (square), in pure helium (triangle) and in the mixture of helium (97%) and argon (3%) (circle).

The above results show that the anisotropy of the interaction more clearly manifests itself in the vertical direction, which is in agreement with the theoretical and numerical analysis of the problem.<sup>19–21</sup>

### III. CHARACTERISTICS OF A DISCHARGE IN THE GAS MIXTURE

#### A. Electron drift

During the drift in an electric field, electrons gain energy from the electric field; due to Joule heating the electron gains the average energy  $Q_{EW} = eEW$  per unit time, where  $e$  is the electron charge,  $E$  is the electric field strength, and  $W$  is the drift velocity. The energy gained by the electron is lost in elastic collisions with atoms, is expended on excitation of atomic levels and ionization; furthermore, electrons take away or gain energy during recombination,  $Q_{EW} = Q_{ea} + Q_{ex} + Q_{ion} + Q_{rec}$ . The right-hand side is the sum of the corresponding average energy losses of one electron per unit time (during recombination, the electron can also gain energy, e.g., triple electron-ion recombination).<sup>22–28</sup>

The electron energy distribution function (EEDF) in an alternating electric field with amplitude  $E_a$  approximately

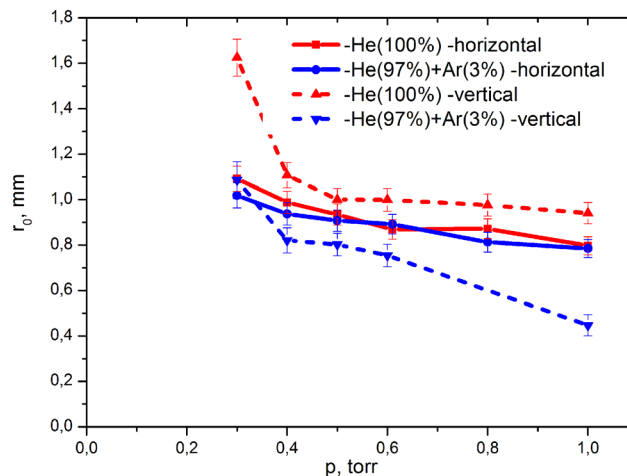


FIG. 5. The average distance between the nearest particles as a function of gas pressure in the horizontal and vertical planes in pure helium and helium-argon mixture.

corresponds to the distribution function in a constant field  $E = E_a/\sqrt{2}$ .<sup>26</sup> Therefore, we analyze EEDF with a drift in a homogeneous constant field. If the increase in the electron velocity between elastic collisions exceeds the velocity of atoms, then the solution to the Boltzmann equation in the two-term approximation can be written as<sup>22–24</sup>

$$f_0(v) = A \exp\left(-\frac{3m}{M}\left(\frac{mN}{eE}\right)^2 \int_0^v c^2 \sigma_{el}^2(c) dc\right), \quad (1)$$

where constant  $A$  is determined by the normalization condition. When  $\sigma_{el}(c) = \sigma_0(c/c_0)^r$ , the integral in Eq. (1) can be calculated. If the frequency of collisions is constant,  $\sigma_{el}(c) = \sigma_0(c/c_0)^{-1/2}$ , the distribution (1) becomes a Maxwellian distribution; if  $\sigma_{el}(c) = \sigma_0$ , the distribution (1) becomes a Druyvesteyn distribution.

The electron energy equation for an electron drift in a mixture of gases is written as

$$-\left(\frac{eE}{m}\right)^2 \frac{1}{\sigma_0 N_0 c} \frac{df_0}{dc} = 3mc^2 f_0 \sum_k \frac{\sigma_k N_k}{M_k} + \sigma_0 N_0 c \langle C^2 \rangle \frac{df_0}{dc}. \quad (2)$$

Introducing the cross section of elastic collisions between electrons and atoms as  $\sigma_0 = \sum_k \sigma_k$  and denoting the fractional concentration of the  $k$ -th species as  $\omega_k = N_k/N_0$ , where the total number density of atoms is  $N_0 = \sum_k N_k$  (the sum runs over all gas species), we rewrite Eq. (2) as

$$(V^2 + \langle C^2 \rangle) \frac{df_0}{dc} = -3mc^2 f_0 \sum_k \frac{\sigma_k \omega_k}{\sigma_0 M_k}, \quad (3)$$

where  $V = eE/m\sigma_0 N_0 c$  is the increase in the electron energy between elastic collisions. The solution to this equation has the form

$$f_0(v) = A \exp\left(-m \int_0^v \sum_k \frac{\sigma_k \omega_k}{\sigma_0 M_k} \frac{3cdc}{V^2 + \langle C^2 \rangle}\right). \quad (4)$$

The calculation was performed using the Monte Carlo method similar to that used in Ref. 8. After each collision, the electron equation of motion in the constant field was integrated and, according to known cross sections of elastic and inelastic processes, the probability of either event was determined. It was assumed that:

- (1) Gas atoms have the Maxwellian velocity distribution and do not change their temperature due to collisions with electrons.
- (2) Elastic electron–atom collisions occur as hard sphere collisions, i.e., isotropic scattering in the center-of-mass system occurs during collision, and the collision cross section depends on the energy of relative electron and atom motion.
- (3) The loss of electrons for atomic level excitation is irreplaceable, i.e., it is assumed that excited atoms lose the

excitation energy in the mode of volume de-excitation and metastable atoms diffuse across the boundaries of the volume under consideration.

- (4) During electron-impact ionization, the electron incident on the atom loses the energy equal to the sum of the ionization energy and the kinetic energy of the second electron. Hence, its energy after an ionization event is  $\varepsilon'_1 = \varepsilon_1 - I - \varepsilon'_2$ . The energy of the first electron equiprobably takes all possible values: where  $0 < R < 1$  is a random number; accordingly, the energy of the second electron is  $\varepsilon'_2 = (\varepsilon_1 - I)(1 - R)$ .
- (5) The processes of electron and atom recombination, excited level quenching, and resonant radiation transport do not change electron energies.

Table I presents kinetic characteristics of electron drift in pure helium (run No.1), helium–argon mixtures (runs 2–5), and pure argon (run 6). The table presents the drift velocity, the average energy, and energy balance characteristics, i.e., energy expenditure on excitation and ionization of different gas components.

Computer simulations show that the energy expenditures on ionization of helium and argon are comparable at 0.2% of argon concentration, and at 1% of argon the energy expenditure on argon ionization is 6 times higher than that on helium ionization. The change in argon concentration does not significantly affect the mean electron energy, but in the energy balance, the energy expenditure on excitation of helium atoms is significant. Therefore, it is necessary to keep in mind the possibility of a rather strong influence of metastable helium atoms on the electron velocity distribution due to super elastic collisions with excited helium atoms.

Figure 6 shows EEDF for various concentrations of argon atoms in the helium–argon mixture: the solid curve corresponds to the drift in pure helium; the solid curve with bold dots corresponds to pure argon, the dashed curve with circles—to helium with 0.1% argon concentration, the dashed-and-dotted curves—to argon concentration of 1%, 3%, 10%, and 100%, respectively. In all calculations  $E/N = 20$  Td. In the top figure, the EEDF is drawn in the logarithmic scale to demonstrate the “EEDF tails,” in the bottom figure the linear scale is used to demonstrate the effect of argon concentration on the “EEDF body.” In the insert, the mean kinetic energies of electrons  $K = \langle \varepsilon \rangle$  are shown.

The results of calculations give a rather complete picture of the mechanism of influence of small argon additions on the characteristics of electrons in the gas discharge.

TABLE I. Drift characteristics of electrons at  $E/N = 20$  Td.

Run	1	2	3	4	5	6
He, %	100	99.9	99	97	90	0
Ar, %	0	0.1	1	3	10	100
Drift velocity, km/s	44.0	44.0	42.8	40.5	35.5	18.7
Average energy, eV	7.80	7.77	7.5	7.1	6.5	5.7
Percentage of He ionization, %	2.8	2.6	1.7	0.9	0.07	0
Fraction to Ar ionization, %	0	1.3	10.4	21.8	27.2	1.36
Fraction to He excitation, %	76.2	73.8	56.5	31.6	6.02	0
Fraction to Ar excitation, %	0	1.06	8.93	2.19	43.0	90.0

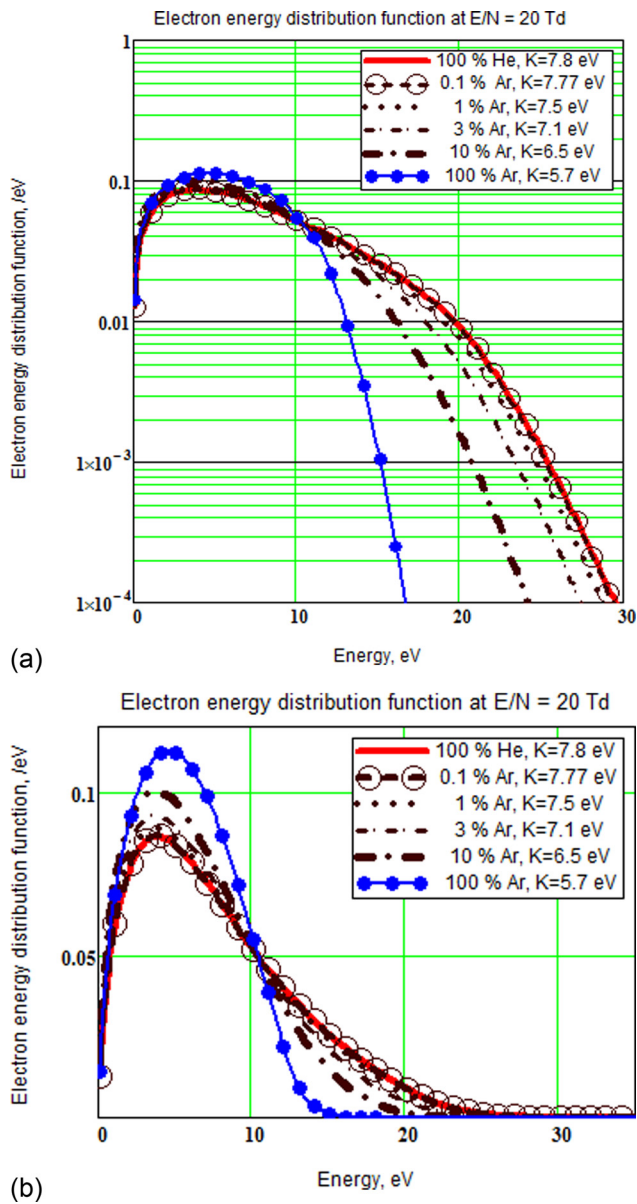


FIG. 6. EEDF for various argon concentrations in helium–argon mixtures.

The most interesting and important fact from practical point of view is a strong increase in the frequency of ionization at low addition of argon (several fractions of a percent). In this case, most argon atoms are ionized, hence, the discharge will mainly contain argon ions.

### B. Ion drift

By analogy with the hydrodynamic approximation, it is often assumed that ion drift is described by the shifted Maxwellian distribution function

$$f_0(\vec{v}) = \left(\frac{m}{2\pi T_i}\right)^{3/2} \exp\left(-\frac{m[(u-W)^2 + v^2 + w^2]}{2T_i}\right). \quad (5)$$

This distribution has two parameters, the average ion velocity  $W$  (drift velocity) and the ion temperature  $T_i$ , which determines thermal spread of ion velocities  $V_T = (T_i/m)^{1/2}$ .

Here, the direction of the field and drift coincides with the  $x$  axis.

The most important practical characteristic of the ion flux is the average kinetic energy of ions connected with the effective ion temperature by the relation

$$\langle \varepsilon \rangle = \frac{1}{2} m \langle v^2 \rangle = \frac{3}{2} T_{eff}. \quad (6)$$

The effective temperature of ions must be taken into account when determining macroscopic characteristics of plasma, e.g., the Debye length.

The introduction of the ion temperature different from the atom temperature can be insufficient to describe the ion distribution function, as the average energies of chaotic motion of ions along and across the field differ in strong fields. Therefore, it is reasonable to introduce two different ion temperatures, i.e., temperatures along  $T_{//}$  and across  $T_{\perp}$  the field. In this case, the average ion energy is given by

$$\langle \varepsilon \rangle = \frac{1}{2} m W^2 + \frac{3}{2} T_i = \frac{1}{2} m W^2 + \frac{1}{2} T_{//} + T_{\perp}. \quad (7)$$

The Mach number defined in gas dynamics as the ratio of the gas velocity to the speed of sound  $M = u/c_s$ , is the most important flux characteristic. As the ion flux characteristic, let us also introduce the effective Mach number  $M_{eff}^2 = mW/T_i$ , where the ion temperature is determined by the equation  $\frac{3}{2} T_i = \langle \varepsilon \rangle - \frac{1}{2} m \langle u \rangle^2$ .

In the strong field, the drift velocity exceeds the thermal velocity of atoms, and the ion and atom temperatures differ significantly. In this case, the use of the thermal velocity of atoms in calculating the Mach numbers of the ion flux leads to a principally incorrect conclusion on the flux nature. In particular, in most studies on dusty plasma, the supersonic ion flux is considered, while as a result of ion heating the ion flux in the intrinsic gas becomes subsonic in case of a significant effect of collisions with charge exchange. The effective Mach number during ion drift in the intrinsic gas turns out to be bounded from the above, as the chaotic motion velocity increases proportionally to the drift velocity. As estimations and calculations show<sup>6,29</sup> (see also the results of calculations, presented below), Mach numbers cannot be larger than two due to ion heating during drift in the intrinsic gas.

Table II presents kinetic characteristics of ion drift, which demonstrate a possibility of achieving large Mach numbers in the case of heavy ion drift in light gas. It was found that the use of mixture of light and heavy gases under typical conditions of experiments with dust structures in plasma makes it possible to suppress ion heating in the electric field and to obtain a supersonic flux with large Mach numbers.

It should be noted that in this case there is a big difference between the temperatures of ions in the distributions parallel (a) and perpendicular (b) to the field. The average kinetic energy of ions is maximal at 3% concentration of argon.

Our calculations lead to the following conclusions about changes in ion drift characteristics caused by addition of helium to argon:

TABLE II. Ion drift characteristics: helium (calculation No. 0) and argon (calculations Nos. 1–6) at  $E/N = 41$  Td.

Run No. – ion type	0 - He <sup>+</sup>	1 - Ar <sup>+</sup>	2 - Ar <sup>+</sup>	3 - Ar <sup>+</sup>	4 - Ar <sup>+</sup>	5 - Ar <sup>+</sup>	6 - Ar <sup>+</sup>
Ar fraction, %	0	0	0.1	1	3	10	100
Drift velocity, km/s	0.94	1.39	1.37	1.24	1.04	0.70	0.16
Temperature $T_{  }$ , K	529	609	700	959	1115	972	363
Temperature $T_{\perp}$ , K	345	470	472	479	478	441	314
Temperature $T_{eff}$ , K	549	3635	3577	3121	2436	1407	371
Mach number $M$	1.21	5.65	5.57	5.04	4.23	2.84	0.64
Mach number $M_{eff}$	1.03	4.26	4.07	3.41	2.75	1.96	0.61

- (1) The drift velocity of argon ions increases by a factor of up to 8.7.
- (2) The highest temperature  $T_{||}$  is reached at a fractional helium concentration of approximately 97%.
- (3) The energy of argon ions (including drift energy) increases by a factor of up to 10.
- (4) The effective Mach number of argon ion flow increases by a factor of up to 7.
- (5) The effect of the parent gas is observed until its concentration is reduced to 0.1%.

The characteristics of ion velocity distribution are also shown in Fig. 7, where the distributions of argon ion velocities along and across the field are presented for several

values of helium concentration in the helium–argon mixture. The results of these calculations suggest a strong influence of gas composition on dust structures in discharge plasmas, making it possible to predict their characteristics due to a supersonic flow regime (Mach cone, anisotropy of interaction between dust grains, etc.).

#### IV. CONCLUSION

The influence of gas composition on plasma parameters and plasma dust structures in the radiofrequency discharge has been studied. The results of experimental studies of dust structures in the RF discharge plasma in the mixture of two types of gases, “light” He and “heavy” Ar, have been analyzed. It has been found that the admixture of a small amount of argon (3%) to helium causes an increase in the interaction anisotropy of dust particles, which is most clearly expressed in a large difference in distances between dust particles in the chain and between chains. The dependence of the mean distance on the gas pressure is presented. It is shown that an increase in gas pressure most strongly affects the distance between dust particles in the chain of the discharge in the mixture. The numerical results show that the ion composition in the discharge is mainly represented by argon ions even if there is only 1% of argon in helium. The drift of argon with lightweight helium gives a strongly anisotropic velocity distribution function. This result is caused by the hypersonic nature of the ion flux in the extrinsic gas. Experimental and numerical results show that even a small admixture of a heavy gas to the light gas drastically changes all characteristics of the plasma, especially the influence of the ion component on dust structures in the plasma.

A more detailed analysis requires calculations of discharge characteristics as a whole, i.e., determination of the electron density and consideration of nonlocality in the electric field distribution. It is also necessary to reconsider the kinetics of dust particle charging, taking into account deviations of the electron distribution function from the Maxwellian distribution function and a decrease in the number of bound ions (due to a decrease in the frequency of ion collisions with intrinsic gas atoms). These problems will be considered in the following studies together with new experimental results.

The results of numerical simulation and theoretical analysis of characteristics of ion and electron drift in gas mixtures enable us to make a conclusion that the use of the discharge in mixtures of various gases offers new prospects in the study of dusty plasma.<sup>13</sup>

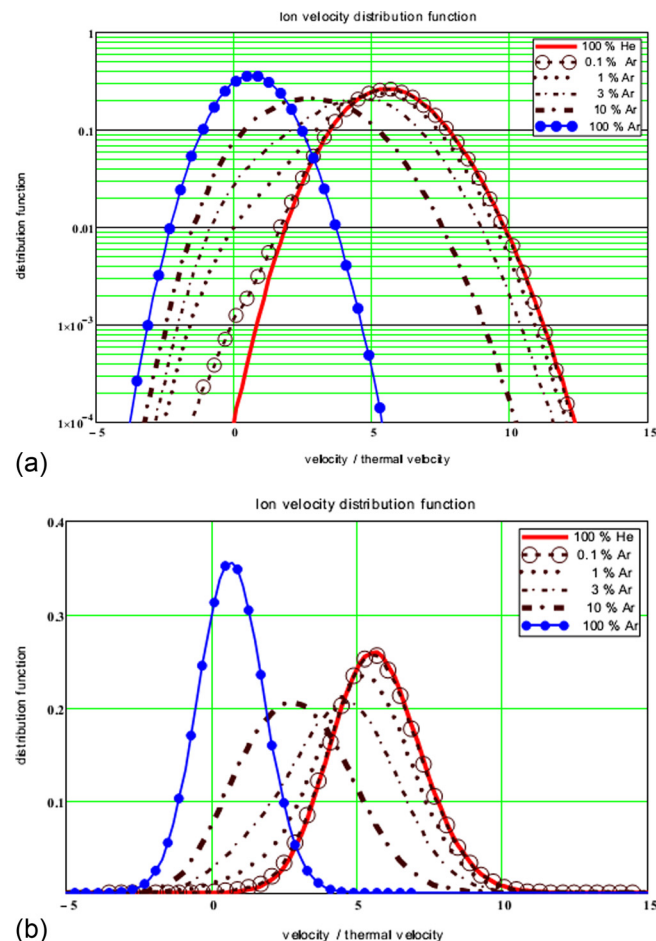


FIG. 7. Ion velocity distribution functions along the field direction for various argon concentrations in the helium–argon mixtures.

## ACKNOWLEDGMENTS

This study was supported by the grant from the Russian Academy of Sciences (Project No. 14-50-00124), the Russian Foundation for Basic Research (Project No. 14-02-00512-a), and the Ministry of Education and Science of the Republic of Kazakhstan (Grant No. 3097/GF4).

- <sup>1</sup>S. A. Maiorov, *Bull. Lebedev Phys. Inst.* **34**, 50 (2007).
- <sup>2</sup>S. A. Maiorov, *Plasma Phys. Rep.* **35**, 802 (2009).
- <sup>3</sup>S. A. Maiorov, R. I. Golyatina, S. K. Kodanova, and T. S. Ramazanov, *Bull. Lebedev Phys. Inst.* **39**, 7 (2012).
- <sup>4</sup>S. A. Maiorov, T. S. Ramazanov, K. N. Dzhumagulova, A. N. Jumabekov, and A. N. Dosbolaev, *Phys. Plasma* **15**, 093701 (2008).
- <sup>5</sup>T. S. Ramazanov, T. T. Daniyarov, S. A. Maiorov, S. K. Kodanova, A. N. Dosbolaev, and E. B. Zhankarashev, *Contrib. Plasma Phys.* **50**, 42 (2010).
- <sup>6</sup>S. N. Antipov, M. M. Vasil'ev, S. A. Maiorov, O. F. Petrov, and V. E. Fortov, *JETP* **139**, 554 (2011).
- <sup>7</sup>E. S. Dzljeva, M. A. Yermolenko, V. Yu. Karasev, S. I. Pavlov, L. A. Novikov, and S. A. Maiorov, *JETP Lett.* **100**, 703 (2014).
- <sup>8</sup>E. S. Dzljeva, V. Yu. Karasev, and A. I. Eikhval'd, *Opt. Spektrosk.* **97**, 107 (2004).
- <sup>9</sup>M. S. Barnes, J. H. Keller, J. C. Forster, J. A. O'Neill, and D. K. Coultas, *Phys. Rev. Lett.* **68**, 313 (1992).
- <sup>10</sup>O. Ishihara, T. Kamimura, K. I. Hirose, and N. Sato, *Phys. Rev. E* **66**, 046406 (2002).
- <sup>11</sup>J. Goree, G. E. Morfill, V. N. Tsytovich, and S. V. Vladimirov, *Phys. Rev. E* **59**, 7055 (1999).
- <sup>12</sup>S. A. Khrapak and V. V. Yaroshenko, *Phys. Plasmas* **10**, 4616 (2003).
- <sup>13</sup>V. E. Fortov, A. G. Khrapak, S. A. Khrapak, V. I. Molotkov, and O. F. Petrov, *Phys.-Usp.* **47**, 447 (2004).
- <sup>14</sup>G. I. Sukhinin and A. V. Fedoseev, *IEEE Trans. Plasma Sci.* **38**, 2345 (2010).
- <sup>15</sup>W. J. Miloch and D. Block, *Phys. Plasmas* **19**, 123703 (2012).
- <sup>16</sup>D. Block, J. Carstensen, P. Ludwig, W. j. Miloch, F. Greiner, A. Piel, M. Bonitz, and A. Melzer, *Contrib. Plasma Phys.* **52**, 804 (2012).
- <sup>17</sup>G. A. Hebner and M. E. Riley, *Phys. Rev. E* **69**, 026405 (2004).
- <sup>18</sup>A. N. Dosbolaev, A. U. Utegenov, T. S. Ramazanov, and T. T. Daniyarov, *Contrib. Plasma Phys.* **53**, 426 (2013).
- <sup>19</sup>S. V. Vladimirov and M. Nambu, *Phys. Rev. E* **52**, 2172 (1995).
- <sup>20</sup>S. A. Maiorov, S. V. Vladimirov, and N. F. Cramer, *Phys. Rev. E* **63**, 017401 (2001).
- <sup>21</sup>S. V. Vladimirov, S. A. Maiorov, and O. Ishihara, *Phys. Plasma* **10**, 3867 (2003).
- <sup>22</sup>L. G. Huxley and R. W. Crompton, *The Diffusion and Drift of Electrons in Gases* (Wiley, New York, 1974), p. 602.
- <sup>23</sup>L. M. Biberman, V. S. Vorob'ev, and I. T. Yakubov, *Kinetics of Nonequilibrium Plasma* (Nauka, Moscow, 1982), p. 140 [in Russian].
- <sup>24</sup>B. M. Smirnov, *Physics of Weakly Ionized Gas in Problems with Solutions* (Nauka, Moscow, 1985), p. 559 [in Russian].
- <sup>25</sup>E. McDaniel and E. Mason, *The Mobility and Diffusion of Ions in Gases* (Wiley, New York, 1973).
- <sup>26</sup>Yu. P. Raizer, *Gas Discharge Physics* (Springer, 1991), p. 449.
- <sup>27</sup>S. A. Maiorov, *Bull. Lebedev Phys. Inst.* **36**, 299 (2009).
- <sup>28</sup>S. A. Maiorov, S. V. Vladimirov, and N. F. Cramer, *Plasma Phys. Rep.* **28**, 946 (2002).
- <sup>29</sup>S. A. Maiorov, *Plasma Phys. Rep.* **32**, 737 (2006).